Study Chloride Barrier Mechanism and Adsorption Kinetics in Self-Healing Cementitious Geo-Materials: A Molecular Dynamics Investigation

Wei Xie[1,2,3], Huiqiu Zhou[1,2,3], Jing Luo[1,2,3], Xianfeng Wang[1,2,3,*], Guolin Wu[4], Qiling Luo[1,2,3], Wujian Long[1,2,3] and Feng Xing[1]

[1]*Guangdong Provincial Key Laboratory of Durability for Marine Civil Engineering, College of Civil and Transportation Engineering, Shenzhen University, Shenzhen 518060, China*

[2]*Shenzhen Key Laboratory for Low-carbon Construction Material and Technology, Shenzhen 518060, China*

[3]*State Key Laboratory of Intelligent Construction and Healthy Operation and Maintenance of Deep Underground Engineering, Shenzhen University, Shenzhen 518060, China*

[4]*Guangzhou Guangjian Construction Engineering Testing Center Co., Ltd., Guangzhou, 510405, China*

Abstract: Chloride-induced corrosion poses a critical threat to the durability of underground structures and geotechnical infrastructure. However, the role of polymer microcapsule wall materials in regulating ion transport within cementitious matrices remains unclear. In this study, a C–S–H/urea–formaldehyde (UF)/NaCl molecular dynamics model was developed to elucidate the barrier mechanism of UF microcapsule walls against chloride ingress. The results show that UF enhances Ca–O correlations in C–S–H, leading to a denser gel structure. UF also forms strong hydrogen bonds with pore water, significantly restricting water mobility and reducing the coordination numbers of Na^+ and Cl^- ions, thereby inhibiting ionic diffusion. Parametric analyses further indicate that increased pore size and temperature accelerate ion mobility, even within typical service conditions. These findings provide atomic-scale evidence that UF microcapsules effectively suppress chloride transport, offering direct implications for enhancing the impermeability and service life of self-healing concrete used in saline geotechnical and underground engineering environments.

Keywords: Polymer microcapsule, Self-healing concrete, Molecular dynamics, Urea-formaldehyde resin, Adsorption, Calcium-silicate-hydrate.

1. INTRODUCTION

With the rapid expansion of urban infrastructure, the engineering focus has increasingly shifted towards the resilience of underground structures and geotechnical systems, such as deep foundations, pile groups, and retaining structures. Unlike superstructures, these geotechnical elements are continuously exposed to complex underground environments where durability and impermeability are paramount. A critical challenge facing these structures is the ingress of aggressive agents, particularly chloride ions, from groundwater and soil, which compromises the integrity of the concrete matrix. To address this, the development of high-performance concrete with self-healing capabilities has emerged as a significant approach. This involves the incorporation of diverse polymers, often in the form of microcapsules, into the cement matrix. These polymers can disperse evenly, merging with cement hydration products to establish novel interface areas. By doing so, they not only aid in stress transfer and crack mitigation but also play a pivotal role in reducing the permeability of the concrete cover, thereby shielding the reinforcement in deep foundations from chloride attack. Consequently, these advancements are vital for elevating the long-term performance of concrete in harsh underground exposure environments [1].

Calcium-silicate-hydrate (C-S-H), the primary hydration product of cement, provides the fundamental binding force and dictates the transport properties of the concrete matrix. In the context of geotechnical engineering, the adsorption and diffusion behaviors of ions within the C-S-H gel pores are critical determinants of a structure's resistance to chemical erosion. Research has increasingly focused on incorporating high-performance composite materials into C-S-H to modify its pore structure. Matsuyama demonstrated the possibility of filling polymers between C-S-H layers, augmenting layer spacing [2, 3]. Li successfully employed rubber and epoxy resin to fill C-S-H gel, noting enhanced binding interactions and elastic modulus [4]. However, for underground structures, the primary concern extends beyond mechanical strength to the barrier performance against ionic transport. Compared to hydrophobic shells like polystyrene, UF exhibits excellent interfacial bonding with the hydrophilic cement paste, alongside the requisite brittleness for trigger sensitivity. Wang *et al*. [5-7] leveraged these properties to integrate

*Address correspondence to this author at the Guangdong Provincial Key Laboratory of Durability for Marine Civil Engineering, College of Civil and Transportation Engineering, Shenzhen University, Shenzhen 518060, China; E-mail: xfw@szu.edu.cn

Received on 12-11-2025 Accepted on 22-12-2025 Published on 29-12-2025

E-ISSN: 3083-3590/25

epoxy-urea-formaldehyde microcapsules into cement-based materials, enabling self-repair of the gel matrix. While this enhances mechanical recovery, the mechanism by which these microcapsule materials (specifically the polymer wall) influence the adsorption and diffusion of chloride ions at the C-S-H interface remains an intricate area that requires deeper investigation.

With advancements in computer technology, molecular dynamics (MD) simulation has emerged as an effective methodology to explore the multifarious properties of gel materials at the molecular scale [8-10], offering superior control over micro-environmental conditions compared to macro laboratory experiments. This is particularly valuable for studying the interactions between aggressive subsurface ions and the cementitious matrix. Hou *et al*. [11] studied the capillary adsorption of NaCl and Na2SO4 solutions in the nanometer channel of the C-S-H coated with epoxy molecules using molecular dynamics methods. Tu *et al*. [12] investigated the impact of salt solutions within gel channels, revealing that the C-S-H interface selectively adsorbs cations and anions through distinct mechanisms—cations via surface electronegativity and anions via electrostatic attraction. Furthermore, numerous researchers have explored the diverse properties of concrete by incorporating various polymers into the C-S-H matrix [13-15]. Nevertheless, research on the mechanisms of using polymer materials in concrete to promote self-healing of cracks has received relatively little attention. As the service life of concrete increases, the issue of crack propagation becomes increasingly significant. Research linking the microcapsule polymer wall materials (such as urea-formaldehyde) to the inhibition of chloride transport in self-healing concrete for geotechnical applications is limited. As the service life of deep foundations and tunnels increases, understanding how these polymers alter the pore environment to mitigate crack propagation and ionic seepage becomes increasingly significant.

Despite the extensive research on polymer-modified cementitious materials, a critical knowledge gap remains regarding the molecular-level barrier mechanisms of Urea-Formaldehyde (UF) resin, particularly in the context of geotechnical applications exposing to saline groundwater. Most existing MD simulations have focused on linear polymers like PEG or PVA for mechanical reinforcement or surface waterproofing. However, the specific interaction mechanism between the cross-linked UF network—widely used as the shell for self-healing microcapsules—and the ionic transport channels within C-S-H gel pores is not yet understood. Crucially, it remains unclear whether UF acts merely as a physical filler or if it actively participates in competitively anchoring aggressive ions (such as chlorides) through functional group interactions. To bridge this gap, this study establishes a composite C-S-H/UF molecular dynamics model to unravel the atomic behavior of ions at the resin-matrix interface. Unlike previous general studies, this work specifically targets the diffusion dynamics under environmental conditions relevant to underground structures (varying pore sizes and temperatures), aiming to provide a theoretical basis for the durability design of piles and tunnels in aggressive saline environments.

This study delves into the influence of urea-formaldehyde resin (UF), a common polymer microcapsule wall material, on the adsorption behavior of ions at the C-S-H surface using molecular dynamics simulation. The research aims to clarify the role of UF in enhancing the durability of geotechnical structures exposed to saline groundwater. By calculating the interatomic radial distribution function (RDF), the ion diffusion coefficient, and the adsorption quantity of ions at the interface, the impact of UF on the adsorption capacity of ions within the matrix interface was analyzed. Furthermore, the influence of varying pore sizes and temperatures—mimicking diverse underground environmental conditions—on ion adsorption was further studied to provide theoretical support for the application of self-healing concrete in deep foundation engineering.

2. METHODOLOGY

The C-S-H structure simulated in this paper is based on Tobermorite 11 Å (T11), a layered structure highly similar to C-S-H, albeit differing in water content and silicon chain polymerization degree [16-20]. First, the monoclinic structure underwent a transformational change into an orthorhombic form. Subsequently, the cell was expanded by 2 × 5 × 1, establishing a C-S-H model with dimensions of A = 21.89 Å, B = 36.18 Å, and C = 76.04 Å. To represent the nanoscale gel pores typical in real geotechnical cementitious matrices, a slit-pore geometry was adopted. Then, the C-S-H model was sectioned along the crystal plane (0 0 1) to generate a pore with a diameter of approximately 40 Å. Although real cement pores exhibit complex tortuosity, this planar slit model effectively captures the essential physicochemical environment of the gel pores where critical interfacial interactions occur. Next, a 1.0 mol/L NaCl solution was introduced into the pore. The chemical potential energy of water was maintained at zero, and the corresponding density was 1.0 g/m^2. Regarding the boundary conditions, periodic boundary conditions (PBC) were applied in all three directions. This setup simulates an infinite periodic system, representing the continuous multi-layered stacking nature of the C-S-H gel network and minimizing surface

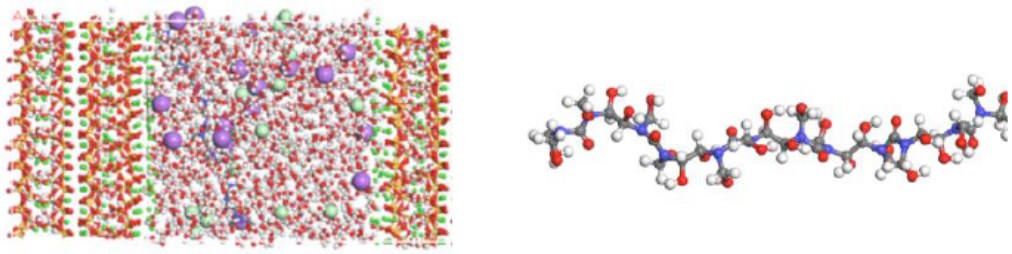

(**a**) (**b**)

Figure 1: Computational Models: (**a**) C-S-H/UF model; (**b**) UF model. (White, red, yellow, dark green, purple, light green, blue, and gray represent hydrogen, oxygen, silicon, calcium, sodium, chlorine, nitrogen, and carbon atoms, respectively.)

truncation effects. Last, to investigate the adsorption mechanism of organic modifiers, UF (as depicted in Figure **1**(**b**)) was placed on the surface of the C-S-H structure, roughly at the position 20 Å along the Z-axis of the entire model. This placement mimics the solid-liquid interface contact anticipated in a hydrated cementitious system. The whole model is illustrated in Figure **1**(**a**).

In this paper, the Materials Studio software was used to conduct molecular dynamics simulation research. After completion of the model, energy minimization was required to obtain the optimal structure. The smart minimizer method is selected as the energy minimizer method, which combines the fastest descent conjugate gradient method and the Newton method to optimize the initial structure. The whole model is simulated under periodic boundary conditions. In the first step, C-S-H and NaCl solutions were fixed, and urea-formaldehyde resin was geometrically optimized. Second, the fixation was removed, and geometric optimization was carried out for the whole model. COMPASS was selected as the force field to optimize the entire model, and the initial model with the lowest energy was obtained. The intermolecular and intramolecular interactions within the simulation system were described using the COMPASS force field [21]. COMPASS is an ab initio force field explicitly parameterized to handle heterogeneous condensed-phase systems. This feature is critical for the present study, which involves complex interfaces between inorganic C-S-H substrates, organic UF polymers, and ionic solutions. Previous studies have validated the accuracy of COMPASS in reproducing the structural and mechanical properties of C-S-H based composites [22, 23]. In the third step, after the equilibrium of C-S-H and NaCl solution, the dynamic relaxation of the whole model was performed by running 200ps under NPT ensemble (N is the number of atoms in the system, P is the pressure and T is the temperature of the simulation) using molecular dynamics method, which the temperature was set to 298 K and the pressure was set to 0 to Make the whole model stress relaxation. Lastly, the entire model was simulated under an NVT ensemble (V is the volume) to get analytical data. Total simulation time was 5000 ps, the timestep was one fs, and the trajectory was output every 5000 steps for subsequent data analysis. To verify the stability of the simulation, thermodynamic parameters were monitored over the 5000 ps trajectory. The energy profiles (Figure **2**) exhibit a flat trend with no significant drift, indicating the system reached a relaxed state. Furthermore, the temperature (Figure **3**) oscillated stably around 298 K throughout the run, confirming that the system maintained thermal equilibrium and justifying the simulation duration.

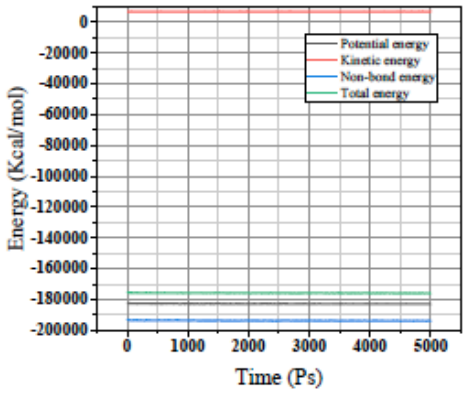

Figure 2: Time evolution of total, potential, and non-bond energies during the MD simulation.

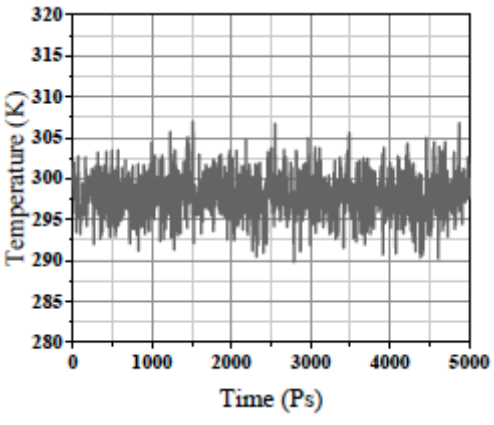

Figure 3: Time dependence of system temperature throughout the 5000 ps production run.

According to numerous studies by scholars [24, 25], the adsorption behavior of water molecules and ions in the C-S-H gel pores is influenced by factors such as pore size, temperature, and whether the polymer is cured. Therefore, this study further investigates and analyzes the effects of pore size and temperature. To investigate the effect of pore size on ion transport, pore widths were set to 20 Å, 40 Å, and 60 Å. These values were specifically selected to represent the realistic range of gel pores within the C-S-H matrix, which serve as the primary pathways for ion diffusion in dense underground concrete structures. According to the microstructural classification of C-S-H, the 20 Å width corresponds to intrinsic gel pores (small gel pores), while the 40 Å and 60 Å widths correspond to larger inter-particle voids or micro-defects. By focusing on this nanoscale range, the study provides an accurate assessment of diffusion resistance in the most limiting phases of the geotechnical barrier, ensuring the results are directly relevant to the durability performance of actual concrete structures.

Additionally, a gel pore model with a pore size of 40 Å was used to study the effect of temperature on adsorption. Three temperature values were chosen: 283 K, 293 K, and 303 K. These values were specifically selected to encompass the typical operational thermal range of geotechnical infrastructure subject to seasonal climatic variations and depth-dependent ground temperatures. Specifically, the lower bound of 283 K (10°C) corresponds to subsurface conditions during winter or in deeper soil strata where temperatures remain relatively low and stable. Conversely, the upper bound of 303 K (30°C) represents near-surface environments during summer or conditions influenced by hydration heat. By analyzing ion transport dynamics across this representative temperature gradient, the study elucidates how environmental thermal fluctuations influence the activation energy of diffusion, thereby providing a theoretical basis for predicting the service life and barrier performance of cementitious materials in complex underground environments.

3. RESULTS AND DISCUSSION

3.1. The Influence of Microcapsule Wall on Ion Adsorption

3.1.1. The Relative Concentration

To intuitively evaluate the specific influence of the microcapsule shell material on ion behavior, an asymmetric slit-pore model was constructed. As illustrated in Figure **1**, the left boundary consists of the UF microcapsule shell surface, while the right boundary consists of a pristine T14 surface, representing the bulk cement matrix. The relative concentration refers to the ratio of the particle number density at a specific distance near the normal direction to the total particle number density within the system. The relative concentration curve can be used to analyze the density distribution information of various particles inside the box. The relative ion concentrations of sodium and chloride ions in the gel channel solution along the parallel Z axis were calculated. As shown in Figure **4**(**a**), sodium ions are primarily concentrated on both sides of the C-S-H surface, at approximately 20 Å and 60 Å. A comparison of the two curves reveals that sodium ions are evenly distributed across both sides of the interface in the C-S-H model without UF, whereas in the C-S-H/UF model, the sodium ion concentration is significantly higher on the side adjacent to the UF. Physically, this asymmetry is attributed to the restructuring of the Electric Double Layer (EDL) at the shell-matrix interface. The urea-formaldehyde chains in the microcapsule wall are rich in nitrogen atoms, which possess lone pair electrons acting as active Lewis base sites. These sites exert a strong electrostatic attraction on cations, effectively creating a "chemical trap" that immobilizes Na+ ions more efficiently than the silicate chains of C-S-H. As shown in Figure **4**(**b**), the relative concentration of chloride ions is mainly concentrated

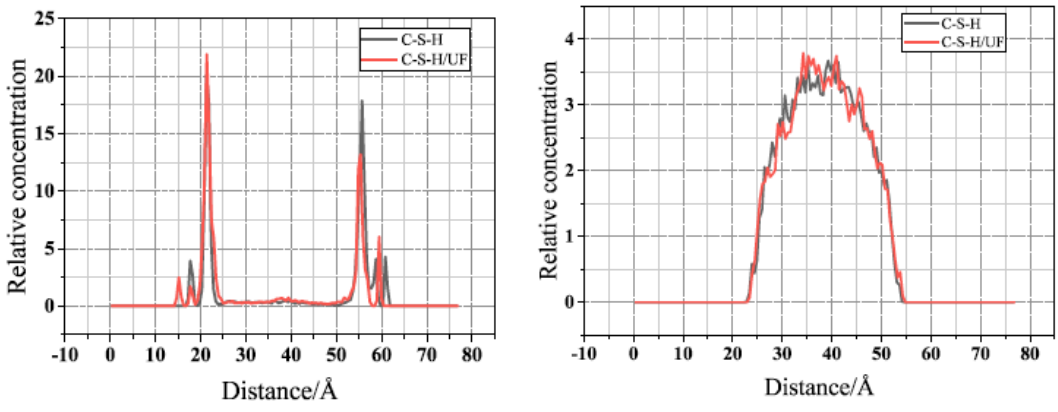

Figure 4: Relative Atomic Concentration: (**a**) sodium ion; (**b**) chloride ion.

between 25 Å and 55 Å, which is also within the range of the gel channel. This indicates that C-S-H has a weak adsorption capacity for chloride ions and suggests the indirect adsorption form of chloride ions on the C-S-H matrix as Os (Oxygen atoms in C-S-H)-Na-Ow (Oxygen atoms in water)-Cl, which also supports the viewpoint of Hou [26]. This finding has significant implications for realistic geotechnical foundations, which often face intrusion from saline groundwater through pores and micro-cracks. Our results suggest that the UF microcapsules serve a dual function. Beyond physically encapsulating healing agents, the shell surfaces dispersed within the foundation's pore network act as active "cation sinks." By electrostatically capturing corrosive ions, the microcapsule shells retard the migration of harmful species into the deep matrix, providing enhanced durability for foundations in aggressive subsurface environments.

3.1.2. Radial Distribution Function

The radial distribution function (RDF) represents the possibility that the central atom appears within a specific range of surrounding atoms and is used to describe the spatial correlation between atoms [15, 27]. The radial distribution function represents the ratio of the local density of B atoms at a distance *r* from an A atom to the bulk average density of B atoms. It quantifies the spatial ordering of B atoms around A atoms. The calculation formula is as follows:

$$g_{AB(r)} = \frac{dN}{\rho 4\pi r^2 \delta r} \quad (1)$$

where *dN* represents the number of class B atoms within the range *r* from A atoms, and *ρ* is the average density of the whole model. When the distance is relatively large to a certain extent, the RDF tends to the average distribution. In addition, the shape of the RDF peak can be used to qualitatively characterize the spatial correlation between atoms in the coordination shell. The sharper the peak, the stronger the consistency of laws between atoms, and the stronger the interaction. The RDF between Ow-Ow (oxygen atoms in solution) can represent the correlation between water molecules in solution to explore the motion characteristics of water molecules in solution. The correlation between Na and Os (oxygen atoms in C-S-H) and the adsorption of ions in solution were analyzed by RDF. The RDF of Ca-Os represents the correlation between calcium ions and oxygen atoms in the C-S-H matrix. The RDF results are shown in Figure **5**. In Figure **5**(**a**), for the C-S-H/UF model, a distinct peak appears at 2.73 Å, whereas for the C-S-H model, the first peak occurs at 2.71 Å. The peak in the

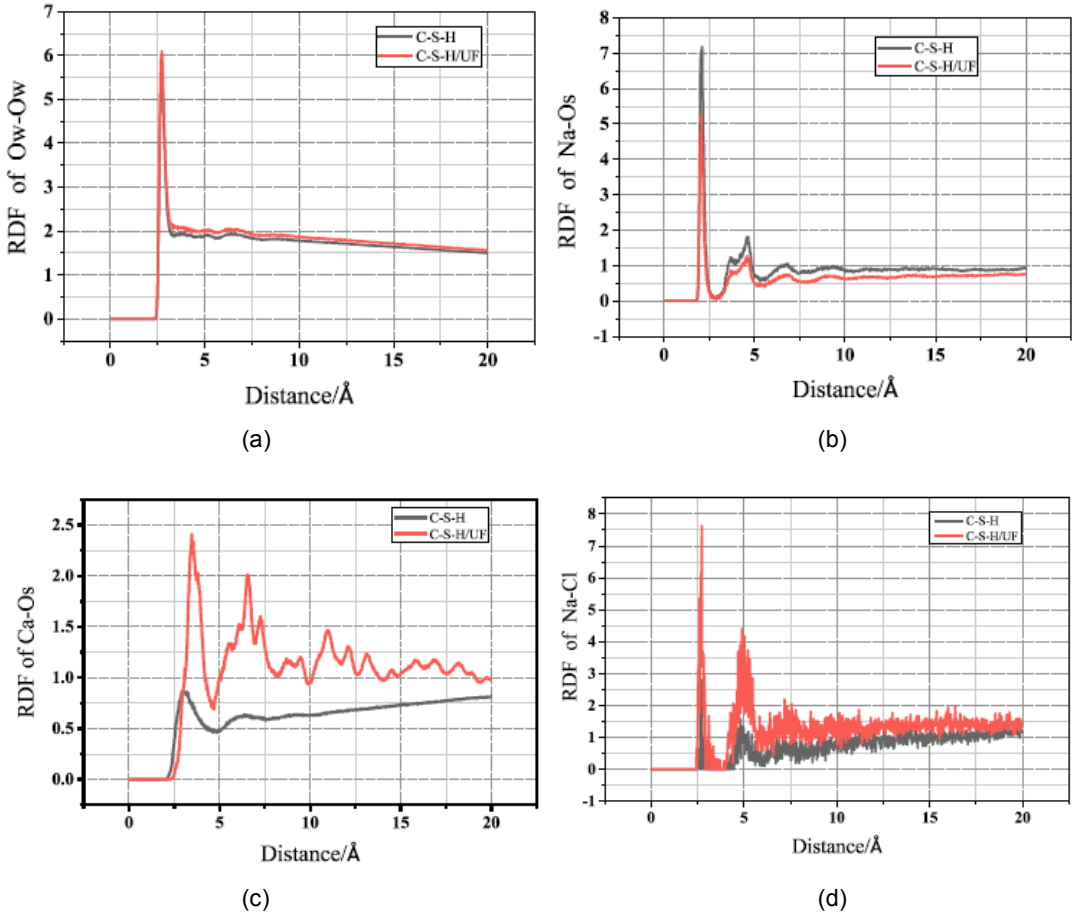

Figure 5: Radial Distribution Function: (**a**) Ow-Ow; (**b**) Na-Os; (**c**) Ca-Os; (**d**) Na-Cl. (Ow: oxygen atoms in water; Os: oxygen atoms in C-S-H).

C-S-H/UF model is more pronounced, indicating that the introduction of UF leads to a higher peak in the radial distribution function (RDF) of water molecules in the solution. In other words, the incorporation of UF enhances the interactions among water molecules. As illustrated in Figure **5**(**b**), the peak positions are identical for both the C-S-H and C-S-H/UF models, but the peak intensity is higher for the C-S-H model. This is because the negatively charged surface of the C-S-H matrix promotes the aggregation of cations. In contrast, the addition of UF hinders the interaction between Na^+ and Os atom [28]. As shown in Figure **5**(**c**), for the RDF of the C-S-H/UF model, the first peak appears at 2.59 Å with a prominent peak, and there are eight pronounced subsequent peaks; while for the C-S-H model, the first peak appears at 3.57 Å with a slight rise, but no prominent following peaks. These indicate that after the addition of UF, the correlation between calcium and oxygen atoms in the C-S-H matrix is more substantial, and the connection is closer, making the gel denser and not conducive to the adsorption of water and ions. From Figure **5**(**d**), the RDF of Na-Cl possesses a sharp peak at 2.73 Å, indicating the Na-Cl ionic pairs of Os-Na-Cl. There is a broad spread peak at 4.97 Å, which represents the hydration layer structure of Na-Ow-Cl ion, and means that the adsorption form of Cl ion on C-S-H matrix is indirect in the way of Os-Na-Ow-Cl. However, compared with the C-S-H model, the peak of the C-S-H/UF model is more prominent, indicating that the adsorption of various ions is stronger after adding UF.

3.1.3. The Coordination Numbers

The coordination number (CN) represents the number of atoms closest to the atom being considered, and it can be calculated by the area under the first peak of the radial distribution function (RDF). The specific formula is shown as Equation (2), where *r1* represents the position of the first peak valley. The coordination numbers of sodium ions, chloride ions, and water molecules in the C-S-H and C-S-H/UF model solutions are calculated and presented in Tables **1** and **2**.

$$\mathrm{n} = 4\pi \int_0^{r_1} r^2 g(r)\, \rho dr \tag{2}$$

From the data in the tables, it can be observed that the average coordination number of sodium ions is 5.195, which is consistent with the results obtained by previous studies (CN= 4-8 [29, 30]), and the average coordination number of chloride ions is 6.793, which also matches previous research findings (CN= 6-8 [29, 30]). It can be observed that CN (Na-C-S-H) > CN (Na-C-S-H/UF) and CN (Cl-C-S-H) > CN (Cl-C-S-H/UF). After the addition of UF, the coordination number of Na and Cl decreased by 0.0483 and 1.133. This shows that the addition of UF can reduce the interaction between Na and Cl with other atoms, respectively.

This reduction in coordination numbers reflects a fundamental alteration in the ion hydration environment and transport mechanism relevant to geotechnical performance. Specifically, sodium ions' kinetic characteristics are heavily influenced by the hydrogen bonding and spatial distribution of surrounding water molecules. The functional groups in the added UF resin, such as NH2 and CHO, form hydrogen bonds with these water molecules, weakening the direct interaction between water and sodium ions and thereby reducing the coordination number. Similarly, the resin functional groups can form complexes with chloride ions and alter the hydrogen bonding of their surrounding water network, further restricting chloride solvation. Crucially, these microscopic interactions effectively "anchor" the ions to the macromolecular resin network. Macroscopically, this atomic-level restriction translates into reduced ion mobility and increased diffusion resistance [31]. Consequently, the addition of UF contributes to lower permeability of the cementitious matrix, enhancing its barrier performance against aggressive ion ingress.

Table 1: Coordination Numbers of Sodium Ions, Chloride Ions, and Water Molecules in the C-S-H Model

	Na	Cl	Os	Ow	Total
Na	/	0.101	0.221	5.114	5.436
Cl	0.092	/	0.011	7.256	7.359
Ow	0.087	0.118	0.208	3.426	3.631

Table 2: Coordination Numbers of Sodium Ions, Chloride Ions, and Water Molecules in the C-S-H/UF Model

	Na	Cl	Os	Ow	Total
Na	/	0.132	0.138	4.653	4.953
Cl	0.717	/	0.027	5.482	6.226
Ow	0.063	0.107	0.188	3.584	3.942

3.1.4. Mean Square Displacement

The mean square displacement (MSD) is used to analyze the motion trajectory of atoms in the model during the simulation process and to represent the displacement of atoms with time. The definition is

$$< r^2(t) >= \frac{1}{N}\sum_{i=1}^{N} <| r_i(t) - r_i(0) |^2> \quad (3)$$

where $r_i(0)$ is the initial position of the *ith* atom, $r_i(t)$ is the position of the *ith* atom at time t, and *N* is the number of atoms in the system. MSD(t) describes the time function of the atom deviating from its initial position. The MSD curves of Ow atoms in the C-S-H model and C-S-H/UF model are shown below. As shown in Figure **6**(**a**), the motion speed of water molecules in the C-S-H model was higher than in the C-S-H/UF model during the simulation process. On the one hand, the added UF made the water molecule in the solution form a hydrogen bond with the UF, which restricted the movement of water molecules; on the other hand, the added UF filled the pores, making the C-S-H pores smaller and inhibiting the activity of water molecules. Figure **6**(**b**) shows that the ion diffusion becomes more intense after UF incorporation. Although the coordination number analysis indicates that UF functional groups interact with Na ions and alter their hydration shells, the dominant factor governing Na mobility is the electrostatic property of the C-S-H substrate. The surface of pure Tobermorite is strongly electronegative, creating deep potential energy wells that firmly "trap" Na ions via electrostatic adsorption, resulting in very low mobility. When UF is added, the resin molecules coat the C-S-H surface. This coating creates a "shielding effect" that blocks the strong electrostatic attraction from the C-S-H surface. While the UF resin does form complexes with Na ions, this resin-ion interaction is significantly weaker than the original surface-ion electrostatic adsorption. Consequently, the addition of UF effectively "liberates" Na ions from the rigid surface-bound state into a relatively more mobile state within the pore solution. Therefore, despite the chemical interaction with UF, the net effect is a reduction in total constraints and an increase in the macroscopic diffusion coefficient. This is consistent with the conclusion of Section 3.1.1.

3.1.5. Diffusion Coefficients

Diffusion coefficients can be used to characterize the motion characteristics of ions in solution to reflect the adsorption of ions on C-S-H gel according to the fluctuation-dissipation theory in non-equilibrium statistical thermodynamics, and the diffusion coefficients of ions are calculated by MSD [32]:

$$D = \frac{1}{6}\lim_{t\to\infty}\frac{d}{dt}\sum_{i=1}^{N} <| r_i(t) - r_i(0) |^2> = \frac{1}{6}\lim_{t\to\infty}\frac{d}{dt}(MSD) \quad (4)$$

According to Figure **6**(**a**), it can be calculated by Equation (4): $D_{C\text{-}S\text{-}H}$ (Ow)=0.205 Å^2/ps, $D_{C\text{-}S\text{-}H/UF}$ (Ow)=0.185 Å^2/ps. The addition of UF reduces the diffusion coefficient of water because the addition of UF leads to the formation of hydrogen bonds between UF and water molecules as shown in Figure **7**, forming a constraint between UF and water molecules and hindering the movement of water molecules.

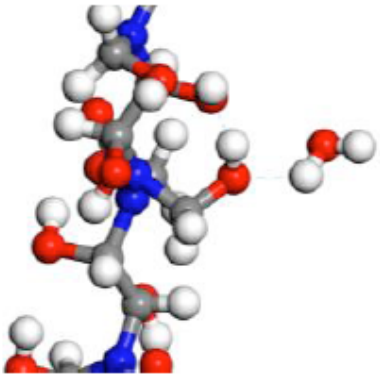

Figure 7: The Hydrogen Bonds between UF and Water Molecules.

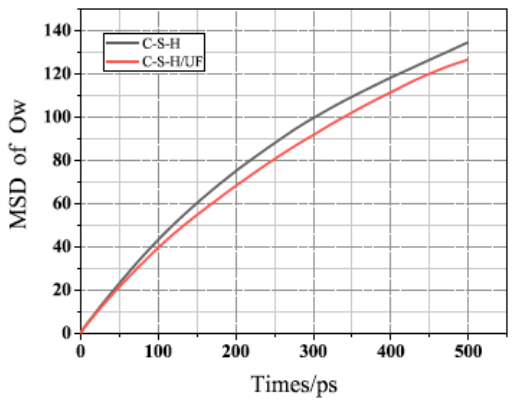

(a)

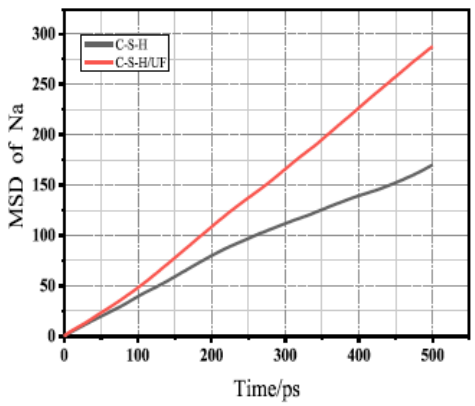

(b)

Figure 6: Mean Square Displacement: (**a**) Ow; (**b**) Na.

According to Figure **5**(**b**), $D_{C\text{-}S\text{-}H}$ (Na)=0.052 $Å^2$/ps and $D_{C\text{-}S\text{-}H/UF}$ (Na)=0.079 $Å^2$/ps were similarly fitted. It can be concluded that the addition of UF increases the diffusion coefficient of sodium ions, which is not conducive to the adsorption of sodium ions at the matrix surface.

3.2. Effect of Pore Size on Adsorption of Water and Ions in C-S-H Gel Channels

3.2.1. Radial Distribution Function

In order to study the local structure of atoms in the solution, the RDFs of water molecules and ions were calculated in gel pores of different sizes. The RDFs provide information about the spatial correlation between water-water, water-ion, and ion-ion interactions.

As shown in Figure **8**(**a**), the first peak of the Ow-Ow RDF is located at around 2.78 Å, representing the closest hydration layer of water molecules. To quantitatively analyze the local structure, coordination numbers (CN) were calculated,as shown at Table **3**. The Ow-Ow CN decreases significantly from 3.87 to 2.22 as the pore size increases from 20 Å to 60 Å. This trend indicates that water molecules in the 20 Å pore are subject to strong confinement, resulting in a tighter local packing compared to larger pores. As the pore size increases, the confinement effect weakens, leading to a reduction in the number of nearest-neighbor water molecules.

Figure **8**(**b**) displays the Na-Ow RDFs for the three pore sizes. Two peaks appear at 2.05 Å and 4.55 Å, indicating the presence of two hydration layers between Na+ ions and water molecules. Quantitatively, the coordination number represents the hydration level of the ions. The Na-Ow CN is 1.41 in the 20 Å pore, increasing to 1.68 and 1.64 in the 40 Å and 60 Å pores, respectively. While the hydration structure is generally stable, the lower CN at 20 Å suggests that the hydration shell of Na+ ions is partially restricted by spatial constraints in the smallest pore. In pores larger than 40 Å, the hydration environment of Na+ remains consistent.

In Figure **8**(**c**), the Ca-Os RDF shows two peaks at 2.47 Å and 4.52 Å. The calculated coordination number exhibits a clear increasing trend with pore size, rising from 2.03 at 20 Å to 3.18 at 60 Å. This indicates that the binding capacity between Ca2+ ions and surface oxygen (Os) sites is enhanced in larger pores. This

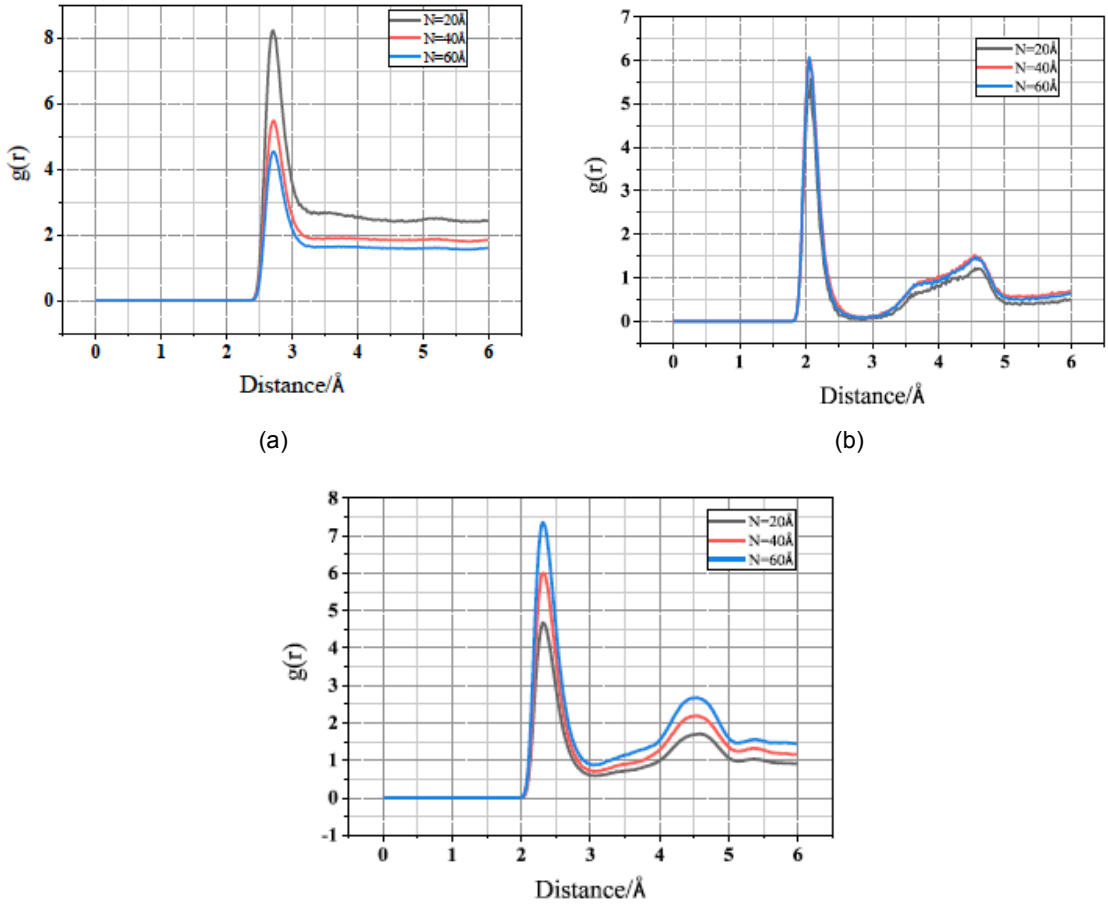

Figure 8: Radial Distribution Function: (a) Ow-Ow; (b) Na-Ow; (c) Ca-Os.

enhancement is attributed to reduced steric hindrance, which allows Ca2+ ions greater orientational freedom to coordinate with surface oxygen atoms, whereas the strong confinement in the 20 Å pore impedes direct interaction.

Table 3: Coordination Numbers of Different Pore Size

	20 Å	40 Å	60 Å
Ow-Ow	3.87	2.64	2.22
Na-Ow	1.41	1.68	1.64
Ca-Os	2.03	2.59	3.18

3.2.2. Mean Square Displacement

Figure **9**(**a**) demonstrates that the MSD of water molecules is larger than that of chloride ions and sodium ions, indicating that water molecules have higher movement speeds compared to various ions in solution. The motion of ions is influenced by factors such as ion concentration, temperature, viscosity, charge magnitude, and ion radius in the solution. In contrast, the movement of water molecules is only influenced by factors such as temperature and viscosity. Generally, smaller solvent molecules have higher movement velocities, while ions have slower movement speeds due to mutual charge repulsion and hindrance from water molecules. The research of Hou *et al*. [26, 33] also found that chloride ions exhibit weaker adsorption capability in C-S-H channels and have higher motion rates than sodium ions.

Figure **9**(**b**) shows that as the pore size increases, the MSD of water molecules gradually increases. This is attributed to larger pore sizes providing more space, resulting in reduced hindrance to the movement of water molecules and allowing them to move more freely. Smaller pore sizes restrict the movement range of water molecules, while larger pore sizes enable water molecules to diffuse and move more freely.

3.3. Effect of Temperature on Adsorption of Water and Ions in C-S-H gel Channels

3.3.1. Radial Distribution Function

In order to investigate the local atomic structure of solutes, the radial distribution functions (RDFs) of water molecules and ions in the gel pores were calculated at different temperatures. The spatial correlations of water-water, water-ion, and ion-ion interactions were analyzed. As shown in Figure **10**(**a**), at three different temperatures, the oxygen atoms in water molecules exhibit a prominent peak at approximately 2.65 Å. To evaluate the variation in local density, coordination numbers were calculated, as shown at Table **4**. The Ow-Ow CN values are 2.53, 2.50, and 2.63 at 283 K, 293 K, and 303 K, respectively. These slight variations suggest that the local structural arrangement of water molecules remains relatively stable within this temperature range, with no drastic disruption to the nearest-neighbor packing.

As shown in Figure **10**(**b**), the Na-Ow RDF exhibits two distinct peaks at approximately 2.51 Å and 4.82 Å, with the second peak being broader and lower than the first. This suggests the presence of an electrostatic interaction between sodium ions and oxygen atoms in water, mediated by the negatively charged oxygen atom, resulting in a prominent peak. The appearance of the second peak often indicates a close interaction between sodium ions and water molecules, such as hydrogen bonding or van der Waals forces, leading to a broader and lower peak position. A quantitative analysis reveals a clear decreasing trend in the coordination number with rising temperature: the Na-Ow CN drops from 3.23 at 283 K to 3.03 at 293 K, and further to 2.63 at 303 K. This reduction indicates that increased temperature enhances the thermal kinetic energy of water molecules, which destabilizes the hydration shell and promotes the detachment of water molecules from the sodium ions, thereby reducing the coordination density. Specifically, as the

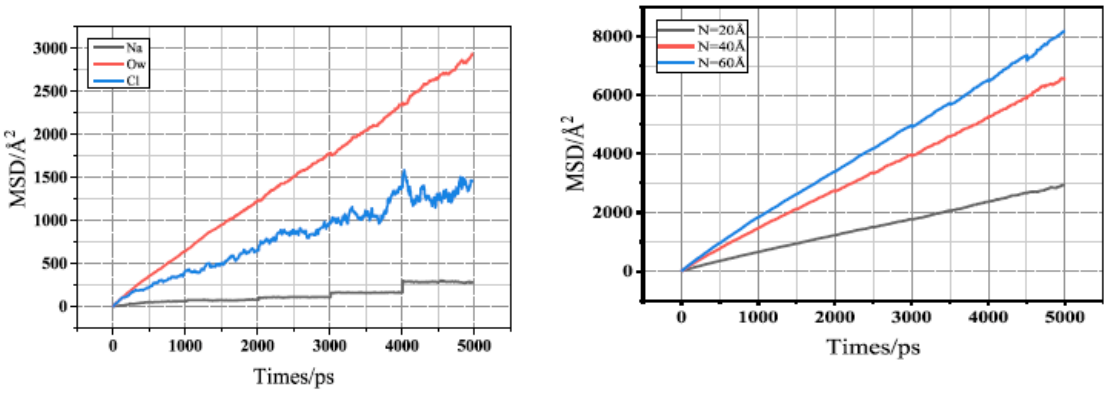

(a) (b)

Figure 9: Mean Square Displacement: (**a**) 40 Å hole model; (**b**) Ow in the models with different pore sizes.

temperature rises, the kinetic energy of water molecules increases, leading to higher mobility and faster diffusion around the ions, thereby reducing the contact time between ions and water molecules. Additionally, as the temperature rises, the average length of hydrogen bonds in water molecules may decrease, causing a change in their arrangement around the ions, further weakening the interaction strength between sodium ions and oxygen atoms in water.

In Figure **10**(**c**), the RDF between calcium ions and oxygen atoms (Os) in C-S-H exhibits four peaks at approximately 2.52 Å, 4.88 Å, 7.21 Å, and 9.8 Å. This complex pattern arises from diverse interactions between calcium ions and oxygen atoms, including electrostatic interactions and other types, such as van der Waals forces. Different peaks often correspond to various interactions, with the first peak representing the formation of chemical bonds between calcium ions and oxygen atoms. In contrast, the subsequent broader peaks may correspond to van der Waals interactions. Despite the temperature variations, the coordination environment of calcium ions is remarkably stable. The calculated Ca-Os coordination numbers are 1.78, 1.78, and 1.79 at 283 K, 293 K, and 303 K, respectively. This consistency suggests that the interaction between Ca2+ ions and surface oxygen sites is governed by strong electrostatic forces. These forces are significantly stronger than the thermal energy fluctuations within this temperature range, resulting in a robust surface coordination structure that is insensitive to temperature changes.

Table 4: Coordination Numbers of Different Temperature

	283 K	293 K	303 K
Ow-Ow	2.53	2.50	2.63
Na-Ow	3.23	3.03	2.63
Ca-Os	1.78	1.78	1.79

3.3.2. Mean Square Displacement

As shown in Figure **11**(**a**), the simulation results indicate an increasing trend in the MSD of chloride ions with increasing molecular structure temperature. This is because the higher temperature increases the kinetic energy of molecules and ions, thereby increasing the motion and diffusion rates of chloride ions. At lower temperatures, the diffusion rate of chloride ions is slow, and their movement is relatively restricted, resulting in smaller MSD values. As the temperature increases, the movement range and speed of chloride ions increase,

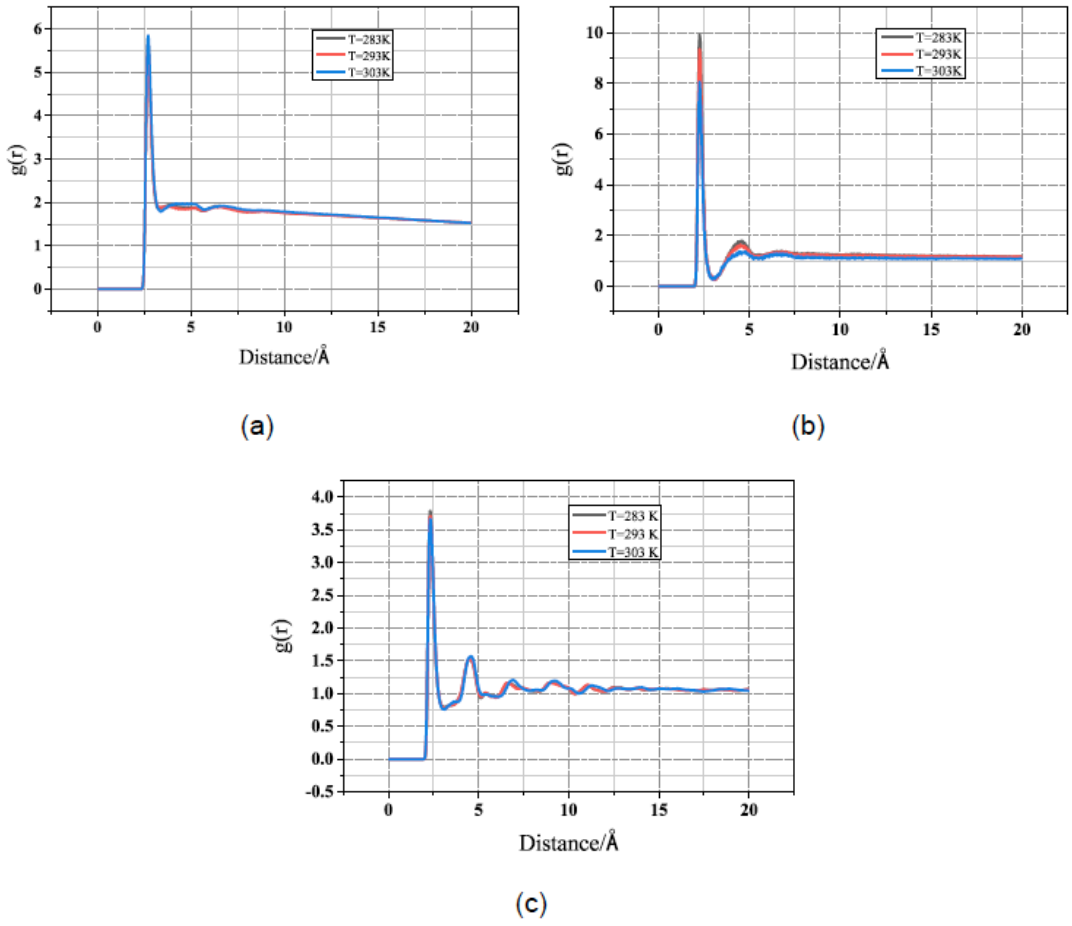

Figure 10: Radial Distribution Function: (**a**) Ow-Ow; (**b**) Na-Ow; (**c**) Ca-Os.

leading to an increase in MSD values. This also reflects that the C-S-H substrate exhibits weak adsorption capacity for chloride ions, and no ion pairs are formed through solid interactions with chloride ions in the solution.

As shown in Figure **11** (**b**), with increasing temperature, the MSD of water also increases. This is because, as the temperature gradually rises, the kinetic energy of water molecules increases, resulting in increased free diffusion and range of motion. Additionally, higher temperatures may weaken the strength of hydrogen bonds between water molecules, further promoting the free diffusion and movement of water molecules and contributing to an increase in the MSD value.

As shown in Figure **11**(**c**), the MSD of sodium ions decreases with increasing temperature. This is because sodium ions in C-S-H are typically bound to hydroxyl groups or calcium ions through adsorption and exchange interactions. When the temperature rises, the interactions between hydroxyl or calcium ions in C-S-H and water molecules weaken, resulting in a decrease in the diffusion rate of surface-adsorbed sodium ions.

3.4. Limitations and Future Perspectives

While this study provides critical molecular-level insights into the barrier mechanisms of C-S-H/UF composites, certain limitations inherent to the Molecular Dynamics (MD) approach must be acknowledged to contextualize the findings for geotechnical applications. First, the spatiotemporal scale of MD simulations is restricted to nanometers and nanoseconds, which differs significantly from the macroscopic dimensions and decadal service life of actual underground structures. Although the derived diffusion coefficients serve as robust comparative indicators, the direct quantitative prediction of long-term macroscopic permeability requires upscaling techniques, such as coupling MD outputs with continuum-based Finite Element Methods (FEM). Second, the pure Tobermorite model used to represent C-S-H is an idealized structure that does not fully capture the chemical heterogeneity, such as aluminum substitution or impurity content, often found in field concrete. Future research should therefore focus on bridging these scales through multiscale modeling and rigorous experimental validation. Specifically, macroscopic rapid chloride migration (RCM) tests and microstructural analyses (*e.g.*, SEM-EDS) are

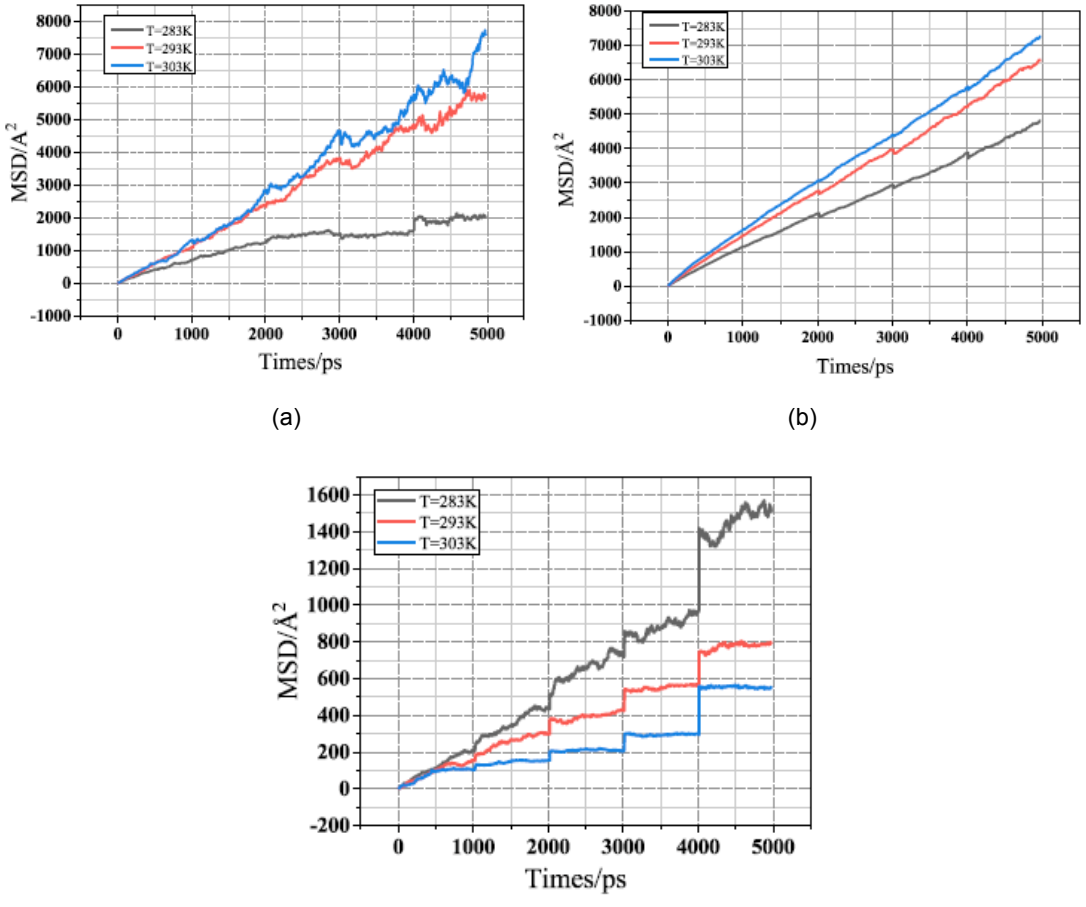

Figure 11: Mean Square Displacement: (**a**) Cl; (**b**) Ow; (**c**) Na.

recommended to verify how the atomic-level "anchoring" effects and pore modifications observed in this simulation translate into the bulk engineering performance of piles and tunnel linings under complex environmental loads.

4. CONCLUSIONS

In this study, a molecular dynamics model was established to elucidate the barrier mechanism of urea-formaldehyde (UF) microcapsules in cementitious matrices. The findings offer critical insights for enhancing the durability of geotechnical infrastructure, such as piles, deep tunnels, and retaining walls, which are frequently exposed to saline groundwater and complex environmental stresses. The key conclusions are summarized as follows:

(1) Chemical Barrier Mechanism: The incorporation of UF forms a dense polymer network that chemically anchors ions and restricts water mobility through hydrogen bonding. This interaction effectively interrupts the continuous hydration shell of aggressive ions (reducing coordination numbers), thereby inhibiting the ingress of corrosive agents. For pile foundations in saline soil, this mechanism provides an enhanced chemical barrier that prolongs service life.

(2) Pore Size and Crack Control: Pore size is a decisive factor controlling diffusion rates. The simulation confirms that ion transport accelerates significantly in larger pores (60 Å) compared to intrinsic gel pores (20 Å). This underscores the engineering necessity of using self-healing microcapsules to seal micro-cracks in underground tunnels and retaining structures, preventing the transition from slow diffusion to rapid convection.

(3) Environmental Sensitivity: Temperature variations within the geotechnical operational range (10–30°C) markedly alter diffusion kinetics. Higher temperatures significantly accelerate chloride migration, indicating that shallow foundations or structures in warmer climates require more robust impermeability design compared to those in deep, thermally stable strata.

Overall, this work substantiates that UF resin acts as an effective active barrier. By mitigating ion transport at the molecular level, it enhances the macroscopic impermeability of concrete, offering a viable solution for protecting critical underground assets against environmental degradation.

FUNDING

This research is financially supported by the National Natural Science Foundation of China (52578304), Shenzhen Natural Science Foundation (JCYJ20240813141827036), Guangdong Provincial Key Laboratory of Durability for Marine Civil Engineering (2020B1212060074), and Shenzhen Key Laboratory for Low-Carbon Construction Material and Technology (ZDSYS20220606100406016).

DATA AVAILABILITY STATEMENT

Data available on request.

CONFLICTS OF INTEREST

The authors declare no conflict of interest.

REFERENCES

[1] Kou, S.C. and Poon, C.S.(2010). Properties of concrete prepared with PVA-impregnated recycled concrete aggregates. Cement & Concrete Composites, 32(8), 649-654. https://doi.org/10.1016/j.cemconcomp.2010.05.003

[2] Hiroyoshi, Matsuyama, J., *et al*.(1999). Synthesis of calcium silicate hydrate/polymer complexes: Part II. Cationic polymers and complex formation with different polymers. Journal of Materials Research, 143389-3396. https://doi.org/10.1557/JMR.1999.0459

[3] [Matsuyama, H. and Young, J.F.(1999). Synthesis of calcium silicate hydrate/polymer complexes: Part I. Anionic and nonionic polymers. Journal of Materials Research, 14(8), 3379-3388. https://doi.org/10.1557/JMR.1999.0458

[4] Li, L., Qin, D., Xu, Z., *et al*.(2022). Study on Strengthening Mechanism of Epoxy Resin/Rubber Concrete Interface by Molecular Dynamics Simulation. Advances in Civil Engineering, 20225100758. https://doi.org/10.1155/2022/5100758

[5] Wang, X., Huang, Y., Huang, Y., *et al*.(2019). Laboratory and field study on the performance of microcapsule-based self-healing concrete in tunnel engineering. Construction and Building Materials, 220(30), 90-101. https://doi.org/10.1016/j.conbuildmat.2019.06.017

[6] Wang, X., Sun, P., Han, N., *et al*.(2017). Experimental Study on Mechanical Properties and Porosity of Organic Microcapsules Based Self-Healing Cementitious Composite. Materials, 10(1), 20. https://doi.org/10.3390/ma10010020

[7] Wang, X., Xing, F., Zhang, M., *et al*.(2013). Experimental Study on Cementitious Composites Embedded with Organic Microcapsules. Materials, 6(9), 4064-4081. https://doi.org/10.3390/ma6094064

[8] Jiang, F., Yang, Q., Wang, Y., *et al*.(2020). Insights on the adhesive properties and debonding mechanism of CFRP/concrete interface under sulfate environment: From experiments to molecular dynamics. Construction and Building Materials, 269(1), 121247. https://doi.org/10.1016/j.conbuildmat.2020.121247

[9] Wang, P., Qiao, G., Guo, Y., *et al*.(2020). Molecular dynamics simulation of the interfacial bonding properties between graphene oxide and calcium silicate hydrate. Construction and Building Materials, 260119927. https://doi.org/10.1016/j.conbuildmat.2020.119927

[10] Qi, C., Manzano, H., Spagnoli, D., *et al*.(2021). Initial hydration process of calcium silicates in Portland cement: A comprehensive comparison from molecular dynamics simulations. Cement and Concrete Research, 149106576. https://doi.org/10.1016/j.cemconres.2021.106576

[11] [Hou, D., Yu, J., Liu, Q.-f., *et al*.(2020). Nanoscale insight on the epoxy-cement interface in salt solution: A molecular dynamics study. Applied Surface Science, 509145322. https://doi.org/10.1016/j.apsusc.2020.145322

[12] Tu, Y., Wen, R., Yu, Q., *et al*.(2021). Molecular dynamics study on coupled ion transport in aluminum-doped cement-based materials. Construction and Building Materials, 295123645. https://doi.org/10.1016/j.conbuildmat.2021.123645

[13] Bahraq, A.A., Al-Osta, M.A., Al-Amoudi, O.S.B., *et al*.(2022). Atomistic simulation of polymer-cement interactions: Progress and research challenges. Construction and Building Materials, 327126881-. https://doi.org/10.1016/j.conbuildmat.2022.126881

[14] Zang, Y., Yang, Q., Wang, P., *et al*.(2022). Molecular dynamics simulation of calcium silicate hydrate/tannic acid interfacial interactions at different temperatures: configuration, structure and dynamic. Construction and Building Materials, 326126820-. https://doi.org/10.1016/j.conbuildmat.2022.126820

[15] Liu, K., Cheng, X., Ma, Y., *et al*.(2020). Analysis of interfacial nanostructure and interaction mechanisms between cellulose fibres and calcium silicate hydrates using experimental and molecular dynamics simulation data. Applied Surface Science, 506144914. https://doi.org/10.1016/j.apsusc.2019.144914

[16] Roland, J.M.P., Akihiro, K., Rouzbeh, S., *et al*.(2009). A realistic molecular model of cement hydrates. Proceedings of the National Academy of Sciences, 106(38), 16102-7. https://doi.org/10.1073/pnas.0902180106

[17] Hamid, S.A.(1981). The crystal structure of the 11 Å natural tobermorite $Ca_{2.25}[Si_3O_{7.5}(OH)_{1.5}]\cdot 1H_2O$. Zeitschrift für Kristallographie, 154(1-4), 189-198. https://doi.org/10.1524/zkri.1981.154.14.189

[18] Xu, S., Wang, Y., Hu, J., *et al*.(2016). Atomic Understanding of the Swelling and Phase Transition of Polyacrylamide Hydrogel. International Journal of Applied Mechanics, 08(07), 1640002. https://doi.org/10.1142/S1758825116400020

[19] Nonat, A.(2004). The structure and stoichiometry of C-S-H. Cement & Concrete Research, 34(9), 1521-1528. https://doi.org/10.1016/j.cemconres.2004.04.035

[20] Nonat, A. and Lecoq, X.(1998). The Structure, Stoichiometry and Properties of C-S-H Prepared by C3S Hydration Under Controlled Condition. Springer Berlin Heidelberg, 197-207. https://doi.org/10.1007/978-3-642-80432-8_14

[21] Sun, H.(1998). COMPASS: An ab Initio Force-Field Optimized for Condensed-Phase ApplicationsOverview with Details on Alkane and Benzene Compounds. The Journal of Physical Chemistry B, 102(38), 7338-7364. https://doi.org/10.1021/jp980939v

[22] Al-Ostaz, A., Wu, W., Cheng, A.H.D., *et al*.(2010). A molecular dynamics and microporomechanics study on the mechanical properties of major constituents of hydrated cement. Composites Part B, 41(7), 543-549. https://doi.org/10.1016/j.compositesb.2010.06.005

[23] Tavakoli, D. and Tarighat, A.(2016). Molecular dynamics study on the mechanical properties of Portland cement clinker phases. Computational Materials Science, 11965-73. https://doi.org/10.1016/j.commatsci.2016.03.043

[24] Dongshuai, H. and Zongjin, L.(2014). Molecular dynamics study of water and ions transport in nano-pore of layered structure: A case study of tobermorite. Microporous and mesoporous materials: The offical journal of the International Zeolite Association, 1959-20.

[25] Youssef, M., Pellenq, J.M., and Yildiz, B.(2011). Glassy Nature of Water in an Ultraconfining Disordered Material: The Case of Calcium-Silicate-Hydrate. Journal of the American Chemical Society, 133(8), 2499-510. https://doi.org/10.1021/ja107003a

[26] Hou, D. and Li, Z.(2014). Molecular Dynamics Study of Water and Ions Transported during the Nanopore Calcium Silicate Phase: Case Study of Jennite. Journal of Materials in Civil Engineering, 26(5), 930-940. https://doi.org/10.1061/(ASCE)MT.1943-5533.0000886

[27] Manzano, H., Moeini, S., Marinelli, F., *et al*.(2012). Confined Water Dissociation in Microporous Defective Silicates: Mechanism, Dipole Distribution, and Impact on Substrate Properties. Journal of the American Chemical Society, 134(4), 2208-2215. https://doi.org/10.1021/ja209152n

[28] Wan, H., Yuan, L., and Yu, Z.(2020). Insight Into the Leaching of Sodium Alumino-Silicate Hydrate (N-A-S-H) Gel: A Molecular Dynamics Study. Frontiers in Materials, 7: https://doi.org/10.3389/fmats.2020.00056

[29] Ohtaki, H. and Radnai, T.(1993). Structure and dynamics of hydrated ions. Chemical Reviews, 93(3), 1157-1204. https://doi.org/10.1021/cr00019a014

[30] Hou, D., Li, D., Yu, J., *et al*.(2017). Insights on Capillary Adsorption of Aqueous Sodium Chloride Solution in the Nanometer Calcium Silicate Channel: A Molecular Dynamics Study. The Journal of Physical Chemistry C, 121(25), 13786-13797. https://doi.org/10.1021/acs.jpcc.7b04367

[31] Li, M., Sun, K., and He, M.(2022). Effects of waterborne epoxy resin on the mechanical properties and microstructure of oil-well cement. Journal of Dispersion Science and Technology, 43(14), 2107-2114. https://doi.org/10.1080/01932691.2021.1915158

[32] Kerisit, S. and Liu, C.(2009). Molecular simulations of water and ion diffusion in nanosized mineral fractures. Environmental Science & Technology, 43(3), 777. https://doi.org/10.1021/es8016045

[33] Zhou, Y., Hou, D., Jiang, J., *et al*.(2016). Chloride ions transport and adsorption in the nano-pores of silicate calcium hydrate: Experimental and molecular dynamics studies. Construction & Building Materials, 126(NOV.15), 991-1001. https://doi.org/10.1016/j.conbuildmat.2016.09.110

https://doi.org/10.65904/3083-3590.2025.01.09